Materials Science, Vol. 21, No. 1, 2003

Exchange coupling field in top, bottom, and dual-type IrMn spin valves coupled to CoFe

J. Y. HWANG, J. R. RHEE*

Department of Physics, Sookmyung Women's University, Seoul 140-742, Korea

A comparative study of $Co_{75}Fe_{25}/Ir_{22}Mn_{78}$ exchange biased top, bottom, and dual-type spin valves is presented. IrMn pinned spin valves were prepared by dc magnetron sputtering onto thermally oxidized Si (111) substrates at a room temperature under a magnetic field of about 100 Oe. For as-deposited top -type spin valves, the magnetoresistance (MR) ratio and exchange coupling field (H_{ex}) were 5.6% and 430 Oe, respectively. For bottom IrMn based spin valves, the H_{ex} values are much higher (H_{ex} = 1180 Oe) while MR ratio (3.6%) is reduced with respect to the top spin valves. The blocking temperatures (T_B) of the top and bottom SV were 250 ºC and 270 ºC, respectively. The results concerning magnetic properties together with structural investigations suggest that H_{ex} is mainly dependent on the quality of fcc (111) crystalline texture while MR ratio is sensitive to both crystalline texture and interface roughness. Dual -type spin valves, with the MR ratio of 7.6% and H_{ex} of 850/510 Oe, showed two exchange loops due to the differences in H_{ex} between the top and bottom pinning layers.

Key words: *spin valve; exchange coupling field; MR ratio; blocking temperature; crystalline texture*

1. Introduction

Various antiferromagnetic (AFM) materials have been investigated in order to obtain higher thermal stability [1, 2] and reliability of the pinned layer for use in spin valve (SV) giant magnetoresistance (GMR) heads in high-density magnetic recording [1, 3, 4]. IrMn has been identified as a promising AFM material for SV due to its high exchange coupling field (H_{ex}), high blocking temperature (T_B), and low critical thickness (~80 Å) [5, 6]. Therefore, exchange coupled IrMn (~80 Å)/CoFe bilayer is suitable for narrow gap head structure [3, 7], since IrMn shows a high H_{ex} at smaller layer thickness than other ordered AFM films, such as NiMn and PtMn [1, 8].

In this paper, we present a fabrication method of $Co_{75}Fe_{25}/Ir_{22}Mn_{78}$ exchange coupled top SV (TSV), bottom SV (BSV) and dual SV by dc magnetron sputtering. We

*Corresponding author, e-mail: jrrhee@sookmyung.ac.kr.

focus on SV performance around the optimal IrMn thickness (~100 Å). The effect of cyclic annealing treatments on the magnetic, magnetoresistive, and structural properties of the devices has also been investigated.

2. Experimental

The GMR/SV films with the structures of top Ta45/$Ni_{80}Fe_{20}$30/$Co_{75}Fe_{25}$20/Cu30 /$Co_{75}Fe_{25}$*t*/$Ir_{22}Mn_{78}$100/Ta45, bottom Ta45/$Ni_{80}Fe_{20}$20/$Ir_{22}Mn_{78}$100/$Co_{75}Fe_{25}$*t*/Cu30/Co_{75} Fe_{25}20/$Ni_{80}Fe_{20}$30/Ta45, and dual Ta45/$Ni_{80}Fe_{20}$20/$Ir_{22}Mn_{78}$100/$Co_{75}Fe_{25}$*t*/Cu30/Co_{75} Fe_{25}20/$Ni_{80}Fe_{20}$30/$Co_{75}Fe_{25}$20/Cu30/$Co_{75}Fe_{25}$*t*/$Ir_{22}Mn_{78}$100/Ta45 (all thicknesses are given in angstroms) were deposited at a room temperature by the dc magnetron sputtering on thermally oxidized Si (111) substrates in a magnetic field of about 100 Oe. In BSV and dual SV, a Ta/$Ni_{80}Fe_{20}$ bilayer was used as a seed layer to obtain the exchange biasing of the overlaying CoFe by IrMn. The base pressure of the process was below 2×10^{-8} Torr and the argon (99.9995%) gas pressure was 2 mTorr. The deposition rates of IrMn, CoFe, and NiFe layers were 0.5~1 Å/s. The crystal structures were investigated by X-ray diffraction (XRD) (CuK_α line). In order to induce large H_{ex} between the IrMn layer and the pinned CoFe layer, a series of annealing cycles was applied under a static magnetic field of 1050 Oe in vacuum furnace with the pressure of 5×10^{-7} Torr. Each annealing cycle consisted of a 1-hour ramp to 250 °C, a 1-hour isothermal annealing at 250 °C and a 1-hour cooling down to a room temperature. The $\Delta R/R$ (MR ratio) was measured by the four-point method at a room temperature, with the magnetic field applied along the direction of H_{ex}. The magnetization curves were measured by a vibrating sample magnetometer (VSM). Atomic force microscopy was used to measure the surface roughness.

3. Results and discussion

3.1. Pinned layer thickness dependence of H_{ex} and MR ratio

Figure 1 demonstrates the pinned CoFe film thickness dependence of H_{ex} and MR ratio for both TSV and BSV annealed at 250 °C for 2 h. The MR ratios of TSV and BSV increase with increasing CoFe pinned layer thickness. The hyperbolic H_{ex} (t_{CoFe}) dependence indicates that IrMn/CoFe bilayers approximately follow the common equation [9] $H_{ex} = J/(M_s \times t)$, where J is interfacial exchange coupling energy, M_s and t are the saturation magnetization and the film thickness of the pinned ferromagnetic layer, respectively. In the remainder of this paper, pinned layer thickness of 12 Å will be applied for all SV.

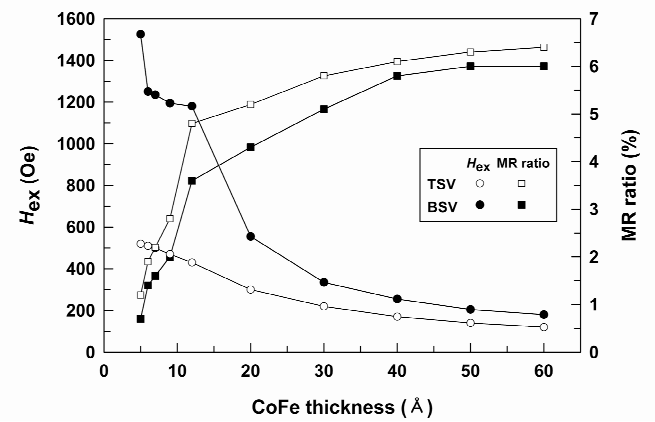

Fig. 1. The pinned CoFe film thickness dependence of the H_{ex} and MR ratio for TSV and BSV after the second annealing

3.2. Structural properties

Typical SV performances with an optimal IrMn thickness of 100 Å are shown in the table. In the as-deposited state, TSV shows a higher MR ratio than BSV system, it exhibits however a poor H_{ex}. For TSV, the annealing for 2 h at 250 °C in vacuum results in an improvement of H_{ex}, while MR ratio is slightly reduced. For BSV, the annealing results in a higher H_{ex} and MR ratio, with H_{ex} being much higher and MR ratio being reduced compared to TSV. Dual SV with MR ratio of 7.6% shows two exchange loops, one at a lower field due to pinning on the top side and a second loop at a higher field due to the bottom side pinning.

Table. Spin-valve parameters for the TSV, BSV, and dual SV evaluated (optimal IrMn thickness of 100 Å)

Spin Valve	R_s (Ω/sq.)	$\Delta R/R$ (%)	H_{ex} (Oe)	H_c (Oe)	H_{int} (Oe)
Top as-deposited	15.26	5.8	380	126	8.5
Top annealed	15.79	5.6	430	100	7.0
Bottom as-deposited	17.38	2.7	680	325	10.5
Bottom annealed	17.16	3.6	1180	150	12.0
Dual annealed	14.32	7.6	850/510	175/140	15.5

Figures 2a, 2b show the X-ray diffraction patterns of the samples: as-deposited and after annealing (two cycles) for the TSV and BSV, respectively. In these figures, we see the preferential (111) peak of the fcc-ordered IrMn accompanied by a peak attributed to the (111) of NiFe and the possible contributions from the (111) of Cu and CoFe. For the as-deposited TSV structure, lattice constants of a = 3.83 Å and 3.62 Å were

obtained from IrMn and CoFe/Cu/ CoFe/NiFe fcc (111) peak positions. For the annealed TSV, an increase in fcc (111) peak intensity indicates an improvement of the crystalline texture induced by annealing. The decrease of the MR ratio may be attributed to higher sheet resistance (R_s) due to interdiffusion, while the higher H_{ex} results from the improved (111) crystalline structure.

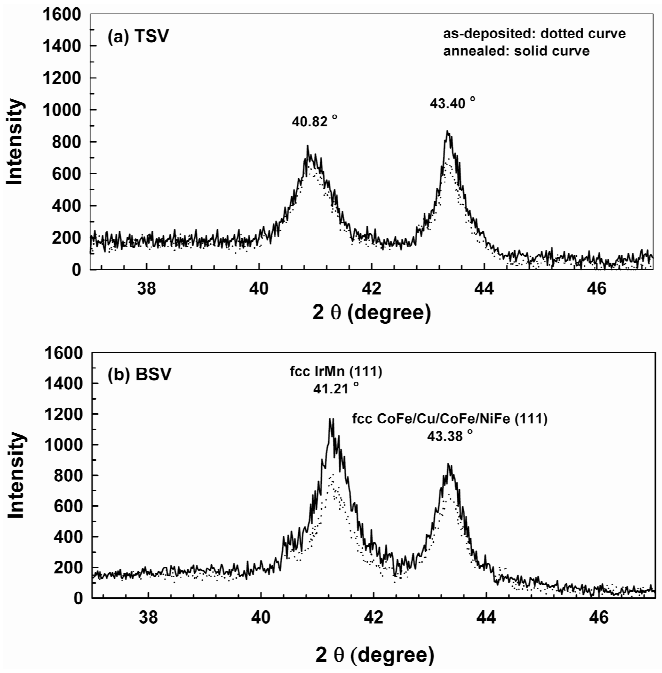

Fig. 2. X-ray diffraction scan patterns for the TSV (a) and BSV (b) in the as-deposited state and after the second annealing

The IrMn (111) peak of annealed BSV shows a higher intensity and a higher 2θ position (a = 3.79 Å) than TSV, while the CoFe/Cu/CoFe/NiFe (111) peak position is unchanged. This indicates a higher perfection of the crystalline texture of IrMn layer in BSV than in TSV structures. In the TSV structure, the IrMn layer grows over a thicker and rougher underlayer of Ta/NiFe/CoFe/Cu/CoFe/NiFe with cumulative roughness [10] which reduces the IrMn texture and a larger average d spacing with a = 3.83 Å.

In contrast to the TSV case, the IrMn layer of BSV has a superior, more compact fcc (111) texture due to its growth on a thin and smooth underlayer of Ta45/NiFe20. The texture of IrMn layer can be further improved by annealing, leading to a more bulk-like microstructure and to higher H_{ex} values. However, since the CoFe/Cu/ CoFe/NiFe layers grow on the rougher IrMn surface with reduced grain size [10, 11] as seen in the (111) peak widths, this leads to a higher R_s, lower MR ratio due to more efficient grain boundary scattering, and a larger H_{int}, interlayer coupling field, compared to the TSV structure.

3.3. Magnetic and MR properties

Magnetic hysteresis loops and major MR curves measured parallel to an easy axis of the BSV structure are shown in Figs. 3 and 4 for as-deposited and annealed (two cycles) samples, respectively. The values of H_{ex} and coercivity (H_c) of the pinned layer of annealed BSV are found to be 1180 Oe and 150 Oe, respectively. A corresponding result is obtained from the major MR curve of Fig. 4a. The room temperature H_{ex} of the BSV film annealed at 250 °C for 2 h was about twice that of the as-deposited one.

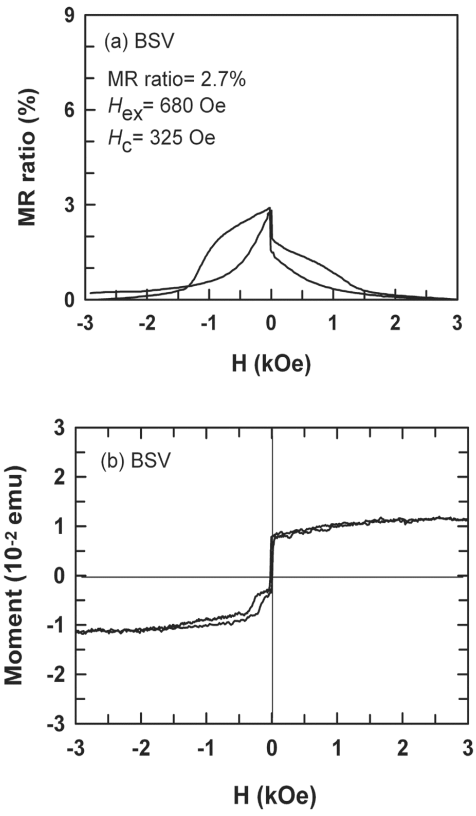

Fig. 3. Major MR (a) and magnetization (b) curves for as-deposited BSV

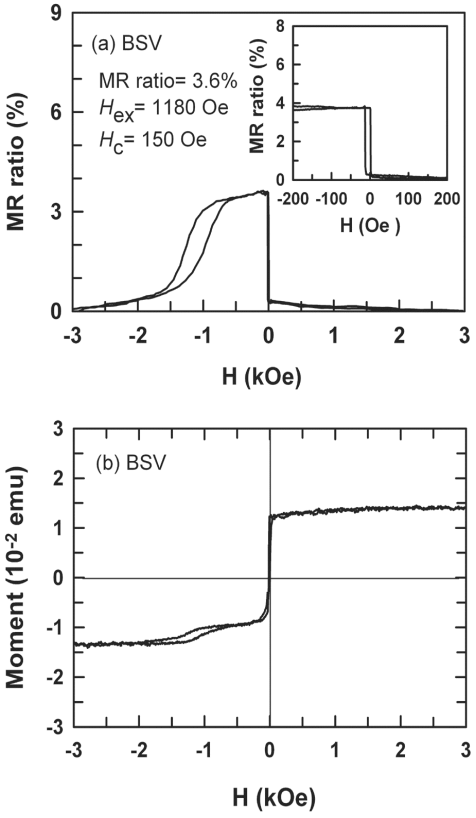

Fig. 4. Major MR (a) and magnetization (b) curves for BSV after the second annealing. The inset in (a) shows minor MR curve

From the minor MR curve (inset in Fig. 4a), it is found that the interlayer coupling field (H_{int}) between the free layer and the pinned layer is about 12 Oe, and the coercive field of the free layer is 5 Oe. In addition, we note that the pinned layer, which is critical for the operation of an SV head, shows stable MR properties. There is no change in its behaviour caused by the fields applied up to about 600 Oe.

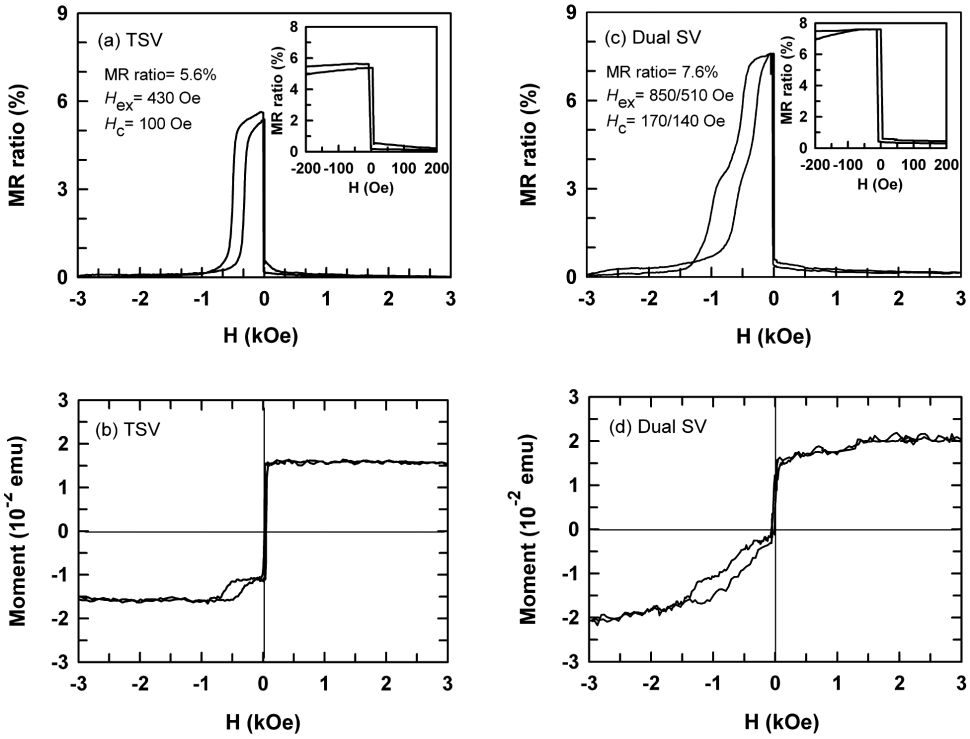

Fig. 5. MR (a) curves and magnetization curves (b) for TSV annealed at 250 ºC for 2h, (c) and (d) – dual SV. The insets in (a) and (c) show minor MR curves

Figure 5 shows the MR and magnetization curves for TSV and dual SV annealed at 250 °C for 2h. The TSV shows a higher MR ratio and lower H_{ex} value. Dual SV, with MR ratio of 7.6% and H_{ex} of 850/510 Oe, shows two exchange loops due to the difference in the H_{ex} between the top and bottom pinned layers.

3.4. Varying the number of annealing cycle

Figure 6 shows the dependence of H_{ex} and MR ratio of the BSV and TSV on the number of annealing cycles. The as-deposited sample shows H_{ex} of 680 Oe and MR ratio of 2.7% for BSV, H_{ex} of 380 Oe and MR ratio of 5.8% for TSV. The H_{ex} and MR ratio of TSV decrease gradually with the number of annealing cycles. For the BSV after one annealing cycle, the H_{ex} and MR ratio increase to about 1180 Oe and 4.3%, respectively. After the second annealing cycle, the MR ratio decreases to 3.6%, and the curves become relatively stable with H_{ex} values of 1180 Oe.

3.5. Thermal stability

For application in SV read head, the H_{ex} should be greater than 300 Oe, and H_{ex} and MR ratio should not be affected by the temperature of 200 ºC during device pro-

duction, or temperature from 200 ºC to 250 ºC produced by electrostatic discharge or sensing current during device operation [12, 13]. This points out the importance of temperature dependence of the H_{ex}. Figure 7 shows the temperature dependence of H_{ex} for TSV and BSV previously subjected to two annealing cycles. The H_{ex} of TSV

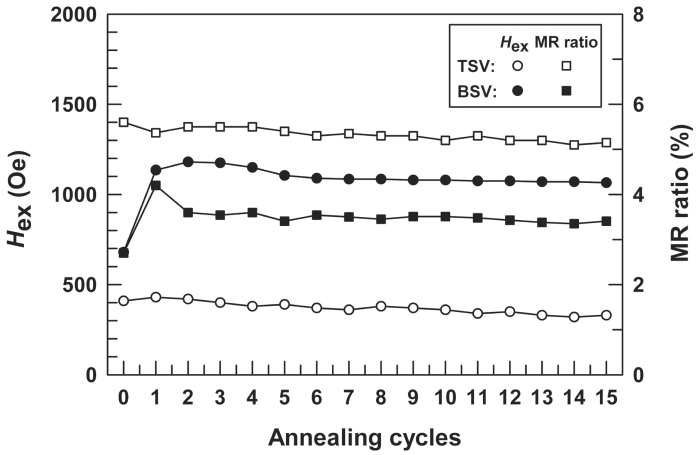

Fig. 6. Annealing cycle dependence of
H_{ex} and MR ratio for the BSV and TSV

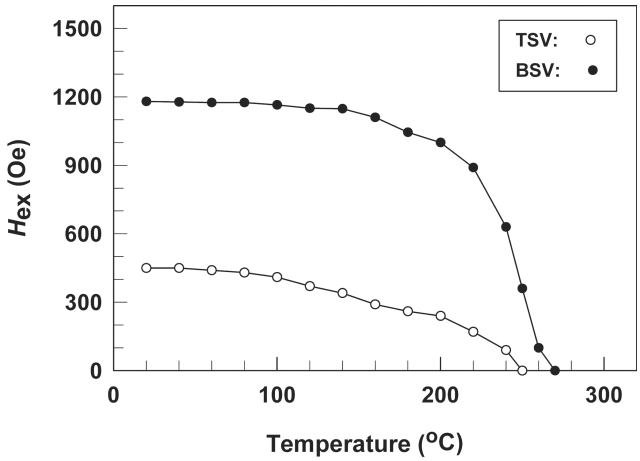

Fig. 7. Temperature dependence of the H_{ex}
for the BSV and TSV after the second annealing cycle

decreases gradually with the temperature increase, reaching zero at 250 °C. The H_{ex} of BSV remains constant at 1180 Oe up to 140 ºC, and then falls to zero at 270 ºC. In particular, the BSV (CoFe spin valves with IrMn) exhibits a higher blocking temperature of 270 °C, and a MR ratio of 3.6%, and an H_{ex} of 1180 Oe, which is the highest ever reported for other post-annealing AFM films, such as NiMn and PtMn [1, 8].

4. Conclusions

Top, bottom, and dual IrMn-based SV were investigated. The BSV shows a lower MR ratio and a higher H_{ex} than the TSV. The high H_{ex} has been attributed to a better IrMn (111) texture with smaller lattice constant (a = 3.79 Å). The reduced MR ratio is attributed to rougher interfaces in the CoFe/Cu/CoFe/NiFe layers with reduced grain size due to a rougher IrMn surface. This interpretation is based on an assumption that H_{ex} depends mainly on the degree of fcc (111) texture, while MR ratio is sensitive to both crystalline texture and interface roughness. Both BSV and TSV structures withstand thermal treatments up to above 250 °C. The pinning field of the BSV remains constant up to 140 °C and then decreases to zero at the blocking temperature of 270 °C, while the pinning field of the TSV decreases gradually and falls to zero at 250 °C. These results suggest that the MR ratios of SV can be enhanced by optimizing the thickness of pinned and free layer for the application of GMR/SV sensor with high thermal stabilities.

Acknowledgements

This work was supported by the 2002 research grants from Sookmyung Women's University.

References

[1] MAO S., GANGOPADHYAYM S., AMIN N., MURDOCK E., Appl. Phys. Lett., 69 (1996), 3593.
[2] CHOI K.L., KIM K.M., LEE N.I., KIM M.Y., RHEE J.R., LEE S.S., HWANG D.G., PARK C.M., IEEE Trans. Magn., 35 (1999), 2943.
[3] FUKE H.N., SAITO K., KAMIGUCHI Y., IWASAKI H., SAHASHI M., J. Appl. Phys., 81 (1997), 4004.
[4] VAN DER HEIJDEN P.A.A., MAAS T.F.M.M., JONGE W.J.M., KOOLS J.C.S., ROOZEBOOM F., ZAAG P.J., Appl. Phys. Lett., 72 (1998), 492.
[5] IWASAKI H., SAITO A.T., TSUTAI A., SAHASHI M., IEEE Trans. Magn., 33 (1997), 2875.
[6] DEVASAHAYAM A.J., SIDES P.J., KRYDER M.H., J. Appl. Phys., 83 (1998), 7216.
[7] FUKE H.N., SAITO K., YOSHIKAWA M., IWASAKI H., SAHASHI M., Phys. Lett., 75 (1999), 3680.
[8] WONG B.Y., MITSUMATA C., PRAKASH S., LAUGHLIN D.E., KOBAYASHI T., IEEE Trans. Magn., 32 (1996), 3425.
[9] LINN T., TSANG C., FONTANA R.E., MAURI D., HOWARD J.K., IEEE Trans. Magn., 31 (1995), 2585.
[10] KOOLS J.C.S., KULA W., MAURI D., LIN T., J. Appl. Phys., 87 (1999), 4466.
[11] ANDERSON G., HUAI Y., MILOSLAWSKY L., J. Appl. Phys., 87 (2000), 6989.
[12] KOS A.B., RUSSEK S.E., KIM Y.K., CROSS R.W., IEEE Trans. Magn., 33 (1977), 3541.
[13] CROSS R.W., KIM Y.K., OTI J.O., RUSSEK S.E., Appl. Phys. Lett., 69 (1996), 3935.

Received 4 December 2002
Revised 31 January 2003